Windborne long-distance migration of malaria mosquitoes in the Sahel

Huestis DL[a], Dao A[b], Diallo M[b], Sanogo ZL[b], Samake D[b], Yaro AS[b], Ousman Y[b], Linton Y-M[f], Krishna A[a], Veru L[a], Krajacich BJ[a], Faiman R[a], Florio J[a], Chapman JW[c], Reynolds DR[d], Weetman D[e], Mitchell R[g], Donnelly MJ[e], Talamas E[h,j], Chamorro L[h], Strobach E[k] and Lehmann T[a]

[a] Laboratory of Malaria and Vector Research, NIAID, NIH. Rockville, MD, USA
[b] Malaria Research and Training Center (MRTC)/Faculty of Medicine, Pharmacy and Odonto-stomatology, Bamako, Mali
[c] Centre for Ecology and Conservation, and Environment and Sustainability Inst., University of Exeter, Penryn, Cornwall, UK and College of Plant Protection, Nanjing Agricultural University, Nanjing, P. R. China.
[d] Natural Resources Institute, University of Greenwich, Chatham, Kent ME4 4TB, and Rothamsted Research, Harpenden, Hertfordshire AL5 2JQ, UK
[e] Department of Vector Biology, Liverpool School of Tropical Medicine, Liverpool, UK
[f] Walter Reed Biosystematics Unit, Smithsonian Institution Museum Support Center, Suitland MD, USA and Department of Entomology, Smithsonian Institution, National Museum of Natural History, Washington DC, USA
[g] Smithsonian Institution - National Museum of Natural History, Washington DC, USA
[h] Systematic Entomology Laboratory - ARS, USDA, Smithsonian Institution - National Museum of Natural History, Washington DC, USA
[j] Florida Department of Agriculture and Consumer Services, Department of Plant Industry, Gainesville FL, USA
[k] Earth System Science Interdisciplinary Center, University of Maryland, College Park, MD, USA

Over the past two decades, control efforts have halved malaria cases globally, yet burdens remain high in much of Africa and elimination has not been achieved even where extreme reductions have occurred over many years, such as in South Africa[1,2]. Studies seeking to understand the paradoxical persistence of malaria in areas where surface water is absent for 3–8 months of the year, suggested that certain *Anopheles* mosquitoes employ long-distance migration[3]. Here, we confirmed this hypothesis by aerial sampling of mosquitoes 40–290 m above ground, providing the first evidence of windborne migration of African malaria vectors, and consequently the pathogens they transmit. Ten species, including the primary malaria vector *Anopheles coluzzii,* were identified among 235 anophelines captured during 617 nocturnal aerial collections in the Sahel of Mali. Importantly, females accounted for >80% of all mosquitoes collected. Of these, 90% had taken a blood meal before their migration, implying that pathogens will be transported long distances by migrating females. The likelihood of capturing *Anopheles* species increased with altitude and during the wet seasons, but variation between years and localities was minimal. Simulated trajectories of mosquito flights indicated mean nightly displacements of up to 300 km for 9-hour flight durations. Annually, the estimated numbers of mosquitoes at altitude crossing a 100-km line perpendicular to the winds included 81,000 *An. gambiae* s.s., 6 million *An. coluzzii*, and 44 million *An. squamosus*. These results provide compelling evidence that millions of previously blood-fed, malaria vectors frequently migrate over hundreds of kilometers, and thus almost certainly spread malaria over such distances. Malaria elimination success may, therefore, depend on whether sources of migrant vectors can be identified and controlled.

In Africa, malaria spans the humid equatorial forest to the semi-arid zones in the north and south. In regions where surface water, essential for larval development, is absent during the 3–8 month dry season, mosquito densities and disease transmission drop dramatically[3–8]. Yet, shortly after the first rain, vector populations surge[6] and transmission recommences. Recent studies suggest that Sahelian *Anopheles coluzzii* survives the long dry season by aestivation (dormancy)[3,6,9–11], whereas *An. gambiae s.s.* (hereafter, *An. gambiae*), and *An. arabiensis* re-establish populations by migration from distant locations where larval sites are perennial[3]. However, direct evidence, including the capture of aestivating adults in their shelters or the recapture of marked-mosquitoes hundreds of kilometers from their release sites, remains elusive.

Mosquito dispersal, hereafter referred to as migration[12], has been extensively studied because it directly impacts disease transmission, the spread of adaptations (e.g., insecticide resistance), and control strategies, such as insecticide barriers[13,14]. Although tracking mosquitoes over large scales has seldom been attempted[13,14], the prevailing view is that the dispersal of malaria mosquitoes does not exceed 5 km[13–16] and the alternative view[17–20] is typically considered to pertain to "accidental events" of minimal epidemiological importance[13]. Nonetheless, the prediction of long-distance migration of anophelines in the Sahel prompted us to question this dogma. Our study is the first to systematically sample insects migrating at high altitude over multiple seasons in Africa to determine if malaria vectors engage in wind-assisted movements, and if so, assess the epidemiological relevance by addressing the following questions: what species are involved? how frequently and at what heights do they fly? how many mosquitoes migrate and how likely are they to carry *Plasmodium*? Then, using simulations, we estimate how far mosquitoes may have travelled and from where.

During 617 aerial sampling nights, we caught 461,100 insects at heights between 40–290 m agl, in four villages in the Sahel of Mali, West Africa (ED Fig. 1), including 2,748 mosquitoes, of which 235 were anophelines (Table 1). These mosquitoes belonged to 10 species: *Anopheles coluzzii*, *An. gambiae*, *An. pharoensis*, *An. coustani*, *An. squamosus*, *An. rufipes*, *An. namibiensis* and three distinct but currently undetermined *Anopheles* (Table 1). The first two are the primary malaria vectors in Africa, with the next four of secondary importance[21]. Mosquitoes were not among the 564 insects captured on 508 control nets (Table 1, and Methods), confirming that these *Anopheles* were intercepted at altitude rather than near the ground during deployment. The maximum anophelines/night was three, indicating that migration occurred over many nights. Consistent with Poisson distributions, the values of the variance to mean ratio were all near one (Table 1 and Supplementary Discussion). Unless otherwise specified, quantitative results presented hereafter refer to the five most abundant *Anopheles* species, represented by >20 individuals (Table 1).

Females outnumbered males by >4:1 (Table 1). Critically, with 87.5% fully gravid, 0.7% semi-gravid, and 2.9% blood-fed, >90% of the anopheline females had taken a blood meal prior to their high-altitude flights (Table 1), suggesting likely exposure to malaria and other pathogens. Although 31% of bloodmeals came from humans, no *Plasmodium*-infected mosquitoes were detected amongst the 23 *An. gambiae s.l.* or the 174 secondary vectors (Table 1). Considering typical rates of *Plasmodium* infections in primary (1–5%) and secondary (0.1–1%) vectors[5,22–24], our results probably reflect the small sample size, with likelihood for zero infected mosquitoes being >30% and >18% (assuming the highest rates in each range), in the primary and secondary vectors, respectively (Supplementary Discussion). Hence, unless infection reduces migratory capacity or migrants are resistant to parasites (there is no evidence for either), *Plasmodium* and other pathogens are almost certainly transported by windborne mosquitoes that may infect people post-migration.

Mosquitoes were intercepted flying between 40 and 290 m agl (Fig. 1a). Overall panel and aerial density increased with altitude, with a significant effect across species on mean panel density ($P<0.037$, $F_{1/24}=4.9$, ED Fig. 2b), suggesting that anopheline migration also occurs >290 m agl. The similar species distributions across years and villages (ED Fig. 2c; non-significant effects of year and village across species, ED Table 1), combined with its marked seasonality (aerial mosquito captures occurred between July–November, peaking between August–October, Fig. 1b, ED Table 1), all attest to the regularity of windborne migration of *Anopheles* mosquitoes.

Using mean aerial densities and wind speeds at altitude (4.8 m/s, Fig. 1c), and conservatively assuming mosquitoes fly in a layer between 50 and 250 m agl (see above), we estimated the nightly expected numbers of migrants crossing a 1-km line perpendicular to the wind direction. Estimates ranged between

27 (*An. gambiae*) and 3,719 (*An. squamosus*, Fig. 1d) per night. When interpolated over a 100-km line joining our sampling sites (ED Figs. 1a, 2c), annual migrations exceeded 80,000 *An. gambiae*, 6.25 million *An. coluzzii*, and 44 million *An. squamosus* in that region alone (Fig 1d). Thus, windborne migration in the Sahel occurs on a massive scale.

For each mosquito capture event, flight trajectories for two- and nine-hour flight durations were estimated using HYSPLIT[25] (using the most accurate assimilated meteorological data available: ERA5), assuming that mosquitoes ascend by their own flight but are passively carried by the wind at altitude (Methods). The mean nightly displacements (straight-line distances) were 30 and 120 km (maxima 70 and 295 km), respectively (Table 2 and Fig. 2). Notably, maximal 9-hour nightly flight displacements ranged between 257–295 km for all anophelines with sample size >20 (Table 2). These backwards trajectories exhibited a south-westerly origin (Rayleigh test; mean bearing = 212°, $r = 0.54$, $P < 0.0001$, Table 2), corresponding to the prevailing winds during peak migration (August–September, Fig. 2). Trajectories of most species originated from a broad arc (>90 degrees, Fig. 2), suggesting migrants emanated from multiple sites across a large region. Migration from this direction fits with the presence of high-density populations due to perennial larval sites and earlier population growth following the monsoon rains. The back-trajectories with a strong northerly component, observed during the sparsely sampled period of October–December (Fig. 2) might indicate southward "return flights", on the Harmattan winds prevailing during this season.

Contrary to the conventional view that dispersal of African anophelines is <5 km[13,15,16,26], our results provide compelling evidence that primary and secondary malaria vectors regularly engage in windborne migration spanning tens to hundreds of kilometers per night. With massive numbers of females that had taken at least one blood-meal, this migration probably involves human *Plasmodium* among other pathogens. Separate outbreaks of malaria in Egypt and Israel have been attributed to *An. pharoensis* traveling over 280 km[17]. Assuming, a conservative[23,27], 1% infection rate in migrating females of *An. coluzzii*, *An. gambiae*, *An. coustani*, and *An. pharoensis* and 0.1% in the remaining anophelines (excluding the unknown *An. sp.* Mali 1 and 2, Supplementary Discussion), a total of 286,700 infected migrant mosquitoes are expected to cross a 100-km line perpendicular to the wind at altitude every year. Accordingly, *An. pharoensis*, *An. coustani*, and *An. coluzzii*, contributed 41%, 25%, and 17%, respectively, to the malaria transmission by infected windborne mosquitoes. Although these estimates are relatively coarse, this suggests that migratory secondary vectors could be a major infection source and should be included in studies of transmission as well as in control programs.

Contrary to our initial prediction[3], *An. coluzzii* was more common than *An. gambiae* among the migrants. This expectation was based on data suggesting that *An. coluzzii* aestivates locally and thus may not require long-distance migration to recolonize the Sahel. Indeed, windborne migration occurs from the end of July to October, well after the surge of Sahelian *An. coluzzii* following the first rain (May–June)[3,6]. The northward and southward oscillations of the Intertropical Convergence Zone during the wet season continually create better mosquito resource-patches with the rains. Additionally, wet-season droughts endanger local mosquito populations every decade or two[28]. Thus, selection pressures to track fresh-water resources by riding the winds that bring rain[29] may explain why Sahelian residents such as *Oedaleus senegalensis* grasshoppers and *An. coluzzii* have a mixed strategy of migration[30] and local dormancy. *Anopheles gambiae*, which presumably recolonizes the Sahel every wet season is relatively rare in Sahelian villages[3], and thus only one specimen was captured by our nets. It may migrate on fewer nights and constitute a smaller fraction of windborne migrants (Supplementary Discussion).

In areas approaching elimination, malaria cases without a history of travel are presumed to represent indigenous transmission. We propose that a substantial fraction of such cases, especially those that occur within ~300 km from high malaria transmission areas, arise from the bites of exogenous-windborne-

infected mosquitoes. For example, north-eastern South Africa has the highest incidence of persistent malaria in the country with many cases not associated with human travel, which are concentrated in an arc extending over ~150 km from the borders with Zimbabwe and Mozambique, where transmission is still high. This area includes the Kruger National Park where roads are scarce and vehicular transport of infected mosquitoes[31] may be hampered. Testing the correlation of such infection events with corresponding winds will help to assess this hypothesis. If confirmed, incorporation of disease control efforts in source populations to minimize or block migration are likely to be an essential element of the elimination strategy.

149 **Table 1. Summary of mosquitoes collected in aerial samples on standard and control panels (2013-2015)**

150

	Standard Panels[a] (N=1,894)											Control Panels[b] (N=508)		
Taxa	Total Captured	Mean Panel Density	L95%CL Poisson[c]	U95%CL Poisson[c]	Max/ Panel	Nightly Presence (%)	Var/Mean ratio	% Female (n)	% Post Blood Feed[d] (n)	% Infected[e] (n)	% Anthro-pophily[h]	Total Captured	Mean Panel Density	Max/ Panel
An. squamosus	100	0.053	0.042	0.063	3	11.02	1.37	76.0 (96)	93.2 (73)	0 (73)	41.1 (17)	0	0	0
An. pharoensis	40	0.021	0.015	0.028	2	6.00	1.08	82.5 (40)	100 (33)	0 (33)	33.3 (6)	0	0	0
An. coustani	30	0.016	0.01	0.022	2	4.38	1.05	88.9 (27)	87.5 (24)	0 (24)	14.3 (7)	0	0	0
An. rufipes	24	0.013	0.008	0.018	2	3.24	1.16	80 (20)	93.8 (16)	0 (16)	0 (4)	0	0	0
An. coluzzii	23	0.012	0.007	0.017	2	3.08	1.16	95.5 (22)	90.5 (21)	0 (21)	100 (1)	0	0	0
An. (Ano.) sp. Mali 1	2	0.001	0	0.003	1	0.32	1	100 (2)	100 (2)	0 (2)	nd	0	0	0
An. gambiae s.s.	1	0.0005	0	0.002	1	0.16	1	100 (1)	100 (1)	0 (1)	nd	0	0	0
An. sp. nr concolor[g]	1	0.0005	0	0.002	1	0.16	1	0 (1)	na[f]	na	na	0	0	0
An. sp. Mali 2	1	0.0005	0	0.002	1	0.16	1	100 (1)	100 (1)	0 (1)	nd	0	0	0
An. namibiensis	1	0.0005	0	0.002	1	0.16	1	100 (1)	100 (1)	0 (1)	nd	0	0	0
Anopheles unidentified	12	0.006	0.003	0.01	1	1.78	0.99	33.3 (6)	100 (2)	0 (2)	nd	0	0	0
Culicinae	2340	1.236	1.185	1.286	22	58.19	4.83	86.4 (1866)	96.7 (1629)	nd	nd	0	0	0
Culicid unidentified	173	0.091	0.078	0.105	8	17.18	1.92	62.9 (116)	91.8 (73)	nd	nd	0	0	0
Total Culicidae	2748	1.451	1.397	1.505	23	64.18	4.92	84.5 (1876)	96.2 (1804)	nd	nd	0	0	0
Total Insects	461100	243.58	242.88	244.29	2601	100	314.75	nd[f]	nd	na	na	564	1.110	31

151

152 [a] Nightly aerial sampling using sticky nets (panels, usually 3/balloon) launched and retrieved at 17:00 and 07:00, respectively. Nets were raised to set altitudes between 40 and
153 290 m above ground (see Methods).

154 [b] Control panels were raised to 40 -120 m agl and immediately retrieved during the launch and retrieval of the standard panels to estimate the number of insects captured
155 during the ascent and descent (see Methods).

156 [c] Estimated using the normal approximation of the Poisson distribution. Low negative values < -0.0001, when a single mosquito/taxon were captured, were rounded to zero.

157 [d] Only a few bloodfed and half-gravid females (see text for percentages) were pooled with gravids to reflect those which were evidently exposed to at least one blood meal. In
158 these mosquito species blood feeding is required for egg development as indicated by the gravid state. Unfed mosquitoes consisted of the rest.

159 [e] Infection with human *Plasmodium* species was tested as described in the Methods.

160 [f] na and nd denote not applicable and not determined, respectively.

161 [g] This species was identified based on male genitalia

162 [h] Identified via PCR (see Methods) with additional confirmations by sequencing. Nonhuman hosts include cow, goat, and possibly unknown rodents.

163

Table 2. Summary of displacement distance and source direction based on 2 and 9 hour flight trajectories of mosquitoes produced using HYSPLIT (see Methods and Figure 2).

	Trajectories: 2-hour flight				Trajectories: 9-hour flight								
Taxa	Trajectories N[a]	Displace mean	Displace 95%CLM	Displace min-max	Trajectories N[a]	Displace mean	Displace 95%CLM	Displace min-max	Hourly Disp. mean[c]	Actual Hourly Disp. Mean[d]	mean Bearing Final[e]	R[f] [bearing]	$P_{[R]}$
An. squamosus	1100	27.7	27-29	2-68	400	109.1	103-115	4-265	13.3	12.1	213	0.516	0.0000
An. pharoensis	440	31.1	30-33	1-65	160	125.3	116-134	24-260	14.7	13.9	214	0.660	0.0000
An. coustani	330	28.5	27-30	2-60	120	125.8	114-138	16-295	14.5	14.0	199	0.270	0.0802
An. rufipes	264	26.1	24-28	2-70	96	109.2	97-121	24-257	12.5	12.1	199	0.454	0.0003
An. coluzzii	253	38.6	37-41	3-69	92	154.1	140-168	47-270	17.3	17.1	217	0.815	0.0000
An. sp. Mali 1	22	20	14-26	6-52	8	94.3	52-136	51-172	10.2	10.5	223	0.947	0.0000
An. gambiae s.s.	11	33.5	ND[b]	ND[b]	4	131.1	ND[b]	ND[b]	15.9	14.6	254	ND[b]	ND[b]
An. sp. nr concolor	11	17.2	ND[b]	ND[b]	4	48.2	ND[b]	ND[b]	8.4	5.4	184	ND[b]	ND[b]
An. sp. Mali 2	11	29.9	ND[b]	ND[b]	4	104.4	ND[b]	ND[b]	13.1	11.6	234	ND[b]	ND[b]
An. namibiensis	11	40.1	ND[b]	ND[b]	4	149.3	ND[b]	ND[b]	16.7	16.6	241	ND[b]	ND[b]
Anopheline Overall	2453	29.4	28.8-30.0	1-70.4	892	118.8	115-123	4-295	14.1	13.2	212	0.540	0.0000

[a] The number of unique nightly trajectories assumes all possible nightly interception times, given flight duration and flight start and end between 18:00 and 06:00, respectively. Thus, for each night with a captured mosquito there were eleven unique 2-hour-flight trajectories and four 9-hour-flight trajectories.

[b] Not determined for species with a single specimen captured.

[c] Hourly displacement between successive 1-hour points along the 9-hour trajectory.

[d] Effective hourly displacement computed by as the quotient of the total 9-hour trajectory displacement by 9.

[e] The mean bearing (angle) between the interception point (zero) and the final point of the 9-hour trajectory computed from the North.

[f] A measure of angular dispersion which varies from 0 (uniform dispersion from all directions) to 1 (a single angle where all points align to.

References (Main Text)

1. WHO | World malaria report 2017. *WHO* (2018).

2. Gething, P. W. *et al.* Mapping *Plasmodium falciparum* mortality in Africa between 1990 and 2015. *N Engl J Med* (2016).

3. Dao, A. *et al.* Signatures of aestivation and migration in Sahelian malaria mosquito populations. *Nature* **516,** 387–390 (2014).

4. Fontenille, D. *et al.* High annual and seasonal variations in malaria transmission by anophelines and vector species composition in Dielmo, a holoendemic area in Senegal. *Am J Trop Med Hyg* **56,** 247–253 (1997).

5. Fontenille, D. *et al.* Four years' entomological study of the transmission of seasonal malaria in Senegal and the bionomics of *Anopheles gambiae* and *A. arabiensis* . *Trans R Soc Trop Med Hyg* **91,** 647–652 (1997).

6. Lehmann, T. *et al.* Aestivation of the African Malaria Mosquito, *Anopheles gambiae* in the Sahel. *Am. J. Trop. Med. Hyg.* **83,** 601–606 (2010).

7. Simard, F., Lehmann, T., Lemasson, J. J., Diatta, M. & Fontenille, D. Persistence of *Anopheles arabiensis* during the severe dry season conditions in Senegal: an indirect approach using microsatellite loci. *Insect Mol.Biol.* **9,** 467–479 (2000).

8. Omer, S. M. & Cloudsley-Thompson, J. L. Dry season biology of *Anopheles gambiae* Giles in the Sudan. *Nature* **217,** 879–880 (1968).

9. Adamou, A. *et al.* The contribution of aestivating mosquitoes to the persistence of *Anopheles gambiae* in the Sahel. *Malar J* **10,** 151 (2011).

10. Mamai, W. *et al.* Monitoring dry season persistence of *Anopheles gambiae* s.l. populations in a contained semi-field system in southwestern Burkina Faso, West Africa. *J Med Entomol* **53,** 130–138 (2016).

11. Yaro, A. S. *et al.* Dry season reproductive depression of Anopheles gambiae in the Sahel. *J. Insect Physiol.* **58,** 1050–1059 (2012).

12. Chapman, J. W., Reynolds, D. R. & Wilson, K. Long-range seasonal migration in insects: Mechanisms, evolutionary drivers and ecological consequences. *Ecology Letters* **18,** 287–302 (2015).

13. Service, M. W. Mosquito (Diptera: Culicidae) dispersal - the long and the short of it. *J. Med. Entomol.* **34,** 579–588 (1997).

14. Service, M. W. *Mosquito Ecology Field Sampling Methods*. (Elsevier Applied Science, 1993).

15. Costantini, C. *et al.* Density, survival and dispersal of *Anopheles gambiae* complex mosquitoes in a west African Sudan savanna village. *Med.Vet.Entomol.* **10,** 203–219 (1996).

16. Toure, Y. T. *et al.* Mark-release-recapture experiments with *Anopheles gambiae s.l.* in Banambani Village, Mali, to determine population size and structure. *Med.Vet.Entomol.* **12,** 74–83 (1998).

17. Garrett-Jones, C. The possibility of active long-distance migrations by *Anopheles pharoensis* Theobald. *Bull. World Health Organ.* **27,** 299–302 (1962).

18. Sellers, R. F. Weather, host and vector--their interplay in the spread of insect-borne animal virus

diseases. *J. Hyg. (Lond).* **85,** 65–102 (1980).

19. Glick, P. A. *The distribution of insects, spieders, and mites in the air*. *United States Department of Agriculture, Technical Bulletin* **673,** (1939).

20. Reynolds, D. R. *et al.* Atmospheric transport of mosquitoes in northeast India. *Med. Vet. Entomol.* **10,** 185–186 (1996).

21. Kyalo, D. *et al.* A geo-coded inventory of anophelines in the Afrotropical Region south of the Sahara: 1898-2016. *Welcome Open Res.* **2,** 57- (2017).

22. Beier, J. C. *et al.* Characterization of malaria transmission by *Anopheles* (Diptera: Culicidae) in western Kenya in preparation for malaria vaccine trials. *J Med Entomol* **27,** 570–577 (1990).

23. Antonio-Nkondjio, C. *et al.* Complexity of the Malaria Vectorial System in Cameroon: Contribution of Secondary Vectors to Malaria Transmission. *J. Med. Entomol* **43,** (2006).

24. Toure, Y. T. *et al.* Perennial transmission of malaria by the *Anopheles gambiae* complex in a north Sudan Savanna area of Mali. *Med Vet Entomol* **10,** 197–199 (1996).

25. Stein, A. F. *et al.* NOAA's HYSPLIT Atmospheric transport and dispersion modeling system. *Bull. Am. Meteorol. Soc.* **96,** 2059–2077 (2015).

26. Verdonschot, P. F. M. & Besse-Lototskaya, A. A. Flight distance of mosquitoes (Culicidae): A metadata analysis to support the management of barrier zones around rewetted and newly constructed wetlands. *Limnologica* **45,** 69–79 (2014).

27. Hay, S. I., Rogers, D. J., Toomer, J. F. & Snow, R. W. Annual *Plasmodium falciparum* entomological inoculation rates (EIR) across Africa: literature survey, Internet access and review. *Trans. R. Soc. Trop. Med. Hyg.* **94,** 113–27 (2000).

28. Nicholson, S. E. The West African Sahel: A review of recent studies on the rainfall regime and its interannual variability. *ISRN Meteorol.* **2013,** 32 (2013).

29. Wilson, K. in *Insect migration: Tracking resources through space and time* (eds. Drake, V. A. & Gatehouse, A. G.) 243–264 (Cambridge University Press, 1995).

30. Pedgley, D. E., Reynolds, D. R. & Tatchell, G. M. in *Insect Migration: Tracking resources through space and time* (eds. Drake, V. A. & Gatehouse, A. G.) 3–30 (Cambridge University Press, 1995).

31. Frean, J., Brooke, B., Thomas, J. & Blumberg, L. Odyssean malaria outbreaks in Gauteng Province, South Africa, 2007 - 2013. *SAMJ South African Med. J.* **104,** 335–338 (2014).

Acknowledgements

We thank the residents of Thierola, Siguima, Markabougou, and Dallowere for their consent to work near their homes and for their wonderful assistance and hospitality. Thanks to Dr. Moussa Keita, Mr. Boubacar Coulibaly, and Ousmane Kone for their valuable technical assistance with field and laboratory operations. We thank Dr. Gary Fritz for consultation on the aerial sampling method using sticky panels; Drs. Dick Sakai, Sekou F Traore, Jennifer Anderson, and Thomas Wellems, Ms. Margie Sullivan, and Mr. Samuel Moretz for logistical support, Drs. Frank Collins and Neil Lobo (Notre Dame University, USA) for support to initiate the aerial sampling project. We thank Drs. Jose' MC Ribeiro and Alvaro Molina-Cruz for reading earlier versions of this manuscript and providing us with helpful suggestions and Drs. Alice

Crawford and Fong (Fantine) Ngan, (NOAA/Air Resources Laboratory and CICS, the University of Maryland) for conversions of the MERRA2 and ERA5 datafiles to HYSPLIT format. This study was primarily supported the Division of Intramural Research, National Institute of Allergy and Infectious Diseases, National Institutes of Health. Rothamsted Research received grant-aided support from the United Kingdom Biotechnology and Biological Sciences Research Council (BBSRC). Y-ML & RM are supported by the U.S. Army. Views expressed here are those of the authors, and in no way reflect the opinions of the U.S. Army or the U.S. Department of Defense. The USDA is an equal opportunity provider and employer. Mention of trade names or commercial products in this publication is solely for the purpose of providing specific information and does not imply recommendation or endorsement by the USDA.

Authors Contributions

The project was conceived by TL and DLH. Field methods and operations were designed by DLH with input from DRR and JWC. Field work, protocol optimization, data acquisition and management, and initial specimens processing including tentative species identification was performed by AD, ASY, MD, SD, and YO and subsequent processing by AK, JF, and LV with inputs from ET and LC. Species identification and molecular analysis of specimens were conducted primarily by Y-ML, RM, AK, and BJK with contributions by DW, RF, and MJD. Data analysis and HYSPLIT simulations were carried out by TL with inputs from all authors, especially RF, BJK, DRR, JWC, ES and Y-ML. BJK mapped simulated trajectories. The manuscript was drafted by TL and revised by all authors. Throughout the project, all authors have contributed key ingredients and ideas that have shaped the work and the final paper.

Competing Interests: All authors declare no competing financial interests.

Author information:

-Laboratory of Malaria and Vector Research, NIAID, NIH. Rockville, MD, USA
Diana L. Huestis, Asha Krishna, Laura Veru, Benjamin J. Krajacich, Roy Faiman, Jenna Florio, & Tovi Lehmann

-Malaria Research and Training Center, Faculty of Medicine, Pharmacy and Odonto-stomatology, Bamako, Mali
Adama Dao, Moussa Diallo, Zana L. Sanogo, Djibril Samake, Alpha S. Yaro, & Yossi Ousmane

-Centre for Ecology and Conservation, and Environment and Sustainability Inst., University of Exeter, Penryn, Cornwall, UK and College of Plant Protection, Nanjing Agricultural University, Nanjing, P. R. China
Jason W. Chapman

-Natural Resources Institute, University of Greenwich, Chatham, Kent ME4 4TB, and Rothamsted Research, Harpenden, Hertfordshire AL5 2JQ, UK
Don R. Reynolds

-Department of Vector Biology, Liverpool School of Tropical Medicine, Liverpool, UK
David Weetman, Martin J. Donnelly

-Walter Reed Biosystematics Unit, Smithsonian Institution Museum Support Center, Suitland MD, USA and Department of Entomology, Smithsonian Institution, National Museum of Natural History, Washington DC, USA
Linton Y-M

-Smithsonian Institution - National Museum of Natural History, Washington DC, USA
Mitchell Reed

-Systematic Entomology Laboratory - ARS, USDA, Smithsonian Institution - National Museum of Natural History, Washington DC, USA
Lourdes Chamorro,

-Florida Department of Agriculture and Consumer Services, Department of Plant Industry, Gainesville FL, USA
Elijah Talamas

-Earth System Science Interdisciplinary Center, University of Maryland, College Park, MD, USA
Ehud Strobach

Correspondence should be addressed to Tovi Lehmann (tlehmann@nih.gov).

Figure 1. Flight altitude, seasonality, wind speed, and abundance of migratory anopheline species. **a)** The relationship of altitude (panel height) and panel- (blue) and aerial- (orange, mosquitoes/10^6 m^3 of air) density for the five most common anopheline species (Table 1). Bubble size is proportional to density (x 10^3 is shown in the bubble), thus no bubble is shown with zero value. The number of sampling nights (Nights) per panel height is shown on the left. **b**) Monthly panel density (N=1,894 panels) for the five most common species (Table 1. Note: values of *An. squamosus* were divided by three to preserve scale) overlaid by the length of migration period (dashed lines). Sampling month of species collected once or twice is shown by letters. **c)** Distribution of mean nightly wind speed at flight height in nights with one or more anopheline collected. Wind speed data were taken from ERA5 database after matching panel height to the nearest vertical layer (Methods). Corresponding box-whisker plot (top) shows the median, mean, quartiles and extreme values overlaid by arrows indicating the mean, 10 and 90, percentiles (red). **d)** The number of mosquitoes per species crossing at altitude (50–250 m agl) imaginary lines perpendicular to wind (see legend). Migrants per night per 1 km (right Y axis) are superimposed on the annual number per 100 km line (left Y axis, Main text).

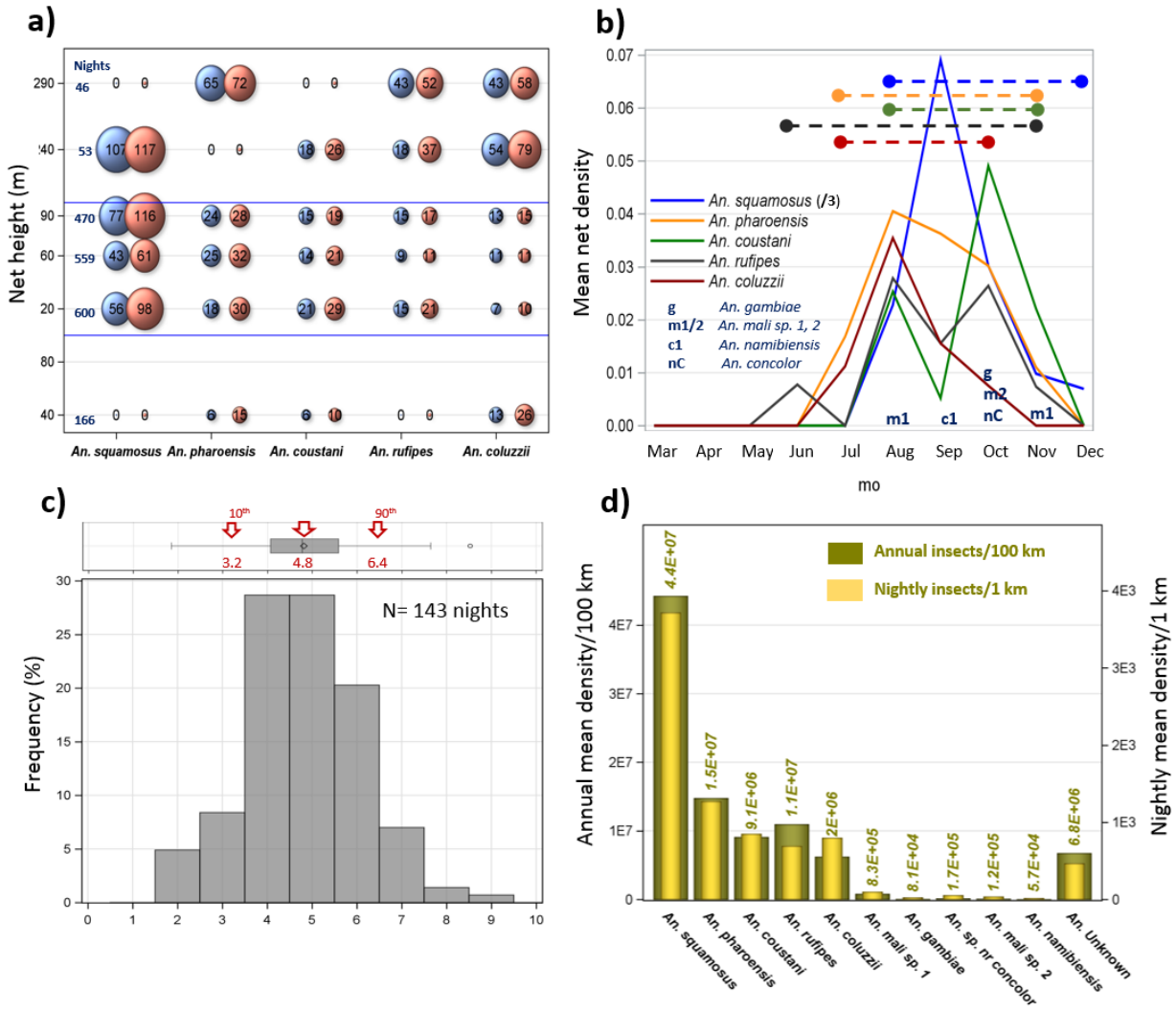

Figure 2. Backward flight trajectories for each anopheles capture event. Backward nine-hour trajectories were estimated by HYSPLIT (Table 2) and overlaid on a map showing parts of Mali and neighboring countries (Map data: Google, Landsat / Copernicus 2019). Each line represents one of 4 simulated trajectories of one (or more) mosquitoes intercepted at that location and night; The area encompassed by the four trajectories is shadowed. Migration season is shown by different line color. *Anopheles* species is indicated above each panel. The seasonal wind rose diagrams reflecting wind conditions at 180 m agl averaged from 2013 to 2015 are shown at the right.

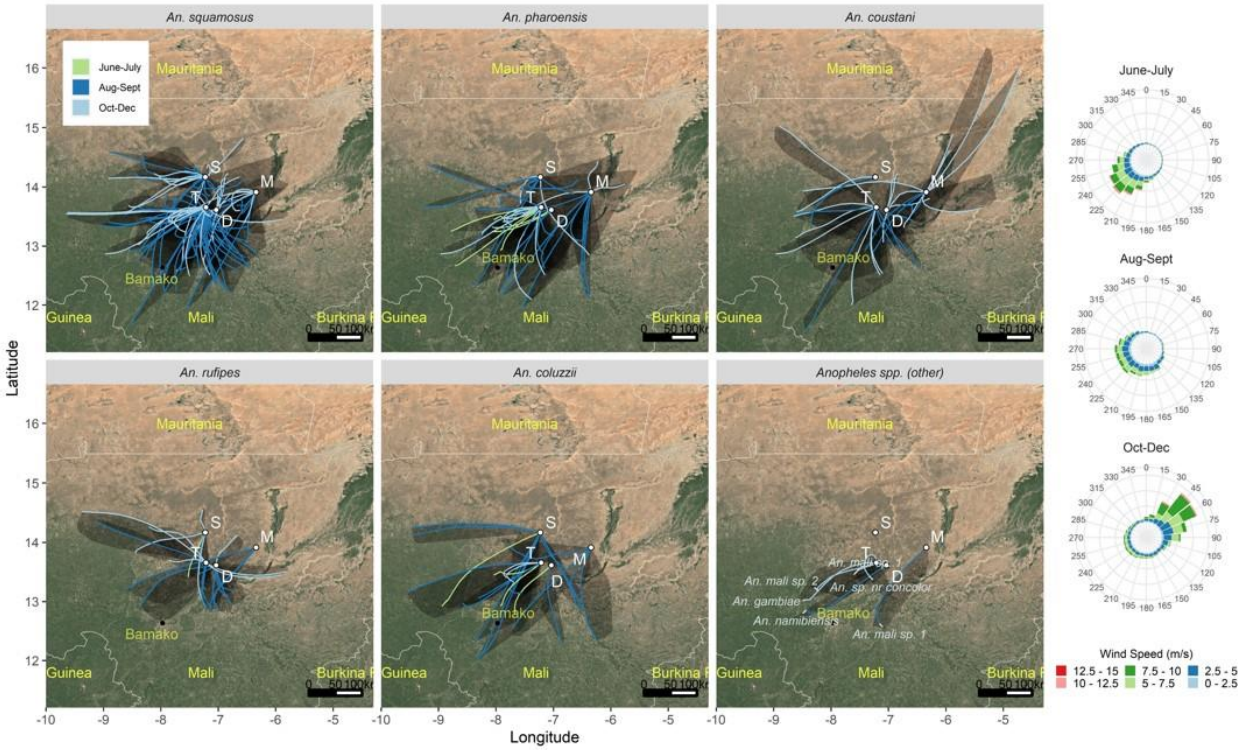

Methods

Study area Aerial sampling stations were located in four Sahelian villages in Mali (Fig. S1): Thierola (13.6586, -7.2147) from March 2013 to November 2015, Siguima (14.1676, -7.2279) from March 2013 to October 2015; Markabougou (13.9144, -6.3438) from June 2013 to April 2015; and Dallowere (13.6158, -7.0369) from July 2015 to November 2015. This study area has been described in detail previously[3,6,9,11,32–34]. Briefly, the region is rural, characterized by scattered villages with traditional mud-brick houses, surrounded by fields. A single growing season (June–October) allows the farming of millet, sorghum, maize, and peanuts, as well as subsistence vegetable gardens. Over 90% of the annual rains fall during this season (~550mm). Cattle, sheep, and goats graze in the savannah that consists of grasses, shrubs, and scattered trees. The rains form small puddles and larger seasonal ponds that usually are totally dry by the end of November. From November until May, rainfall is absent or negligible (total precipitation < 50mm), and by December water is available only in deep wells.

Aerial sampling and specimen processing Aerial sampling stations were placed ~0.5 km from the nearest house of the village in open areas away from large trees. The method of aerial insect collection was adapted from a study on high-altitude mating flights in ants[35]. Rectangular 3 x 1m nets ($3m^2$), cut from a roll of tulle netting (mesh: 8 holes/cm; hole diameter of 1.2 mm), were sewn to form four narrow sleeves 1m apart along the net (ED Fig. 3). A 1m carbon rod was inserted into each sleeve and glued to the net using Duco Cement Glue (Devcon, FL, ED Fig 3). Three nets were spread over each other on a clean large wooden table topped by a 3.5 x 1.5m plywood and coated with a thin film of insect glue (Tanglefoot, Tropical Formula, Contech Enterprises Inc., BC) by rolling a PVC pipe smeared with this glue over them, while applying moderate pressure downward. The pipe was held at each end (from each side of the long table) by two persons and repeatedly rolled (and smeared) until a uniform thin layer of glue coated the net (but did not block its holes). After coating, the sticky nets were immediately rolled individually, and kept in two tightly secured plastic bags indoors, to avoid accidental contact with insects prior to setup.

Prior to the launch, polyurethane balloons (3m in diameter; Mobile Airship & Blimps, Canada, or Lighter than Air, FL, USA), were inflated to full capacity with balloon-grade helium (>98.5%) and topped up to ensure full capacity as needed, usually every 1–3 days based on the balloon condition (ED Fig. 3). Typically, balloons were launched over ~10 consecutive nights per month. The balloon was kept stationary at ~200 m agl by a cord (AmSteel®Blue, synthetic rope sling, Southwest Ocean Services, TX) secured to a $1m^3$ cement block inserted under the ground. The cord then went through a horizontal manually-rotating drum made of a garden-hose reel used for reeling it. A larger 3.3 m diameter balloon (Lighter than Air, FL) was used between July and September 2015, and launched to ~300 m agl.

A team of five trained technicians operated each aerial sampling station. During the launch of a balloon, one team member held the cord under the balloon with heavy-duty gloves and manually controlled its ascent and descent, another controlled the reel, while the other three added or removed the sticky nets to and from their specified positions on the cord. The nets were attached to Velcro panels previously placed on the cord at desirable positions and spaced to fit each of the matching Velcro pieces on the four carbon rods (ED Fig. 3). A knot was made below the top-most Velcro and above the bottom-most Velcro, ensuring that the nets would remain stretched even in strong winds (rather than slip on the cord). Additionally, the team secured the balloons over a “landing patch,” padded by tires covered by a tarpaulin. The balloon was secured to the ground through its main cord by a central hook, at the middle of the landing patch, and by a large tarpaulin that covered it from the top and secured to the ground using 14 large stakes. Team members inspected the nets upon launch to verify that they were free of insects. Upon retrieval of the balloon, the team worked in reverse order and immediately rolled each sticky net

(hereafter, called a panel) and placed it in clean labeled plastic bags, inserted in another bag, each tightened with a cord until inspection.

Each balloon typically carried three sticky nets. Initially, they were suspended at 40, 120, and 160 m agl, but from August 2013, the typical altitude was set to 90, 120, 190 m agl. When the larger balloon was deployed in the Thierola station (August–September 2015), two additional nets were added at 240 and 290 m agl. Balloons were launched approximately 1 hour before sunset (~17:00) and retrieved 1 hour after sunrise (~07:30), the following morning. To control for insects trapped near the ground as the nets were raised and lowered, control nets were raised up to 40 m agl and immediately retrieved (between September and November 2014 the control nets were raised to 120 m agl) during the launch and retrieval operations. The control nets spent 5 minutes in the air (up to 10 minutes when raised to 120 m). Once retrieved they were processed as other nets. Following panel retrieval, inspection for insects was conducted between 09:00 and 11:30 in a dedicated clean area. The panel was stretched between two posts and scanned for mosquitoes, which were counted, removed using forceps, and preserved in 80% ethanol before all other insects were similarly processed and placed in other tubes. Depending on their condition, the sticky panels were sometimes reused the subsequent night.

Species identification Glue attached to the insects was washed off with 100% chloroform. The mosquitoes were gently agitated (<30 sec) to loosen them from one another. Individual mosquitoes were transferred into consecutive wells filled with 85% ethanol. Using a dissecting scope, the samples were morphologically sorted by mosquito subfamily (*Anophelinae, Culicinae*), and tentative identifications to *Anopheles* species /species group undertaken. All *An. gambiae* s.l. visually classified (and two identified based on molecular barcode analysis, see below), were identified to species based on fragment-size differentiation after amplification of the nuclear ITS2 region and digestion of the product[36]. Validation was carried out in LSTM (DW's laboratory) where each specimen was washed with 500µL heptane followed by two further washes with ethanol. DNA was then extracted using the Nexttec (Biotechnologie, GmbH) DNA isolation kit according to manufacturer's instructions. Species identification using a standard PCR method, including all primers[37] with products visualized on 2% agarose gel. *Anopheles gambiae* s.l. samples were further identified to species by SINE insertion polymorphism[38]. In cases where no species-specific bands were detected using the first method, approximately 800 bp region of the mtDNA cytochrome oxidase I genes was amplified using the primers C1_J_2183 and TL2_N_3014[39]. PCR products were purified using the QIAquick PCR-Purification kit (QIAgen) and sequenced in both directions using the original PCR primers by MacroGen Inc. (Amsterdam, Netherlands). Sequences were aligned using CodonCode Aligner (CodonCode Corporation, Dedham, MA) and compared to existing sequences in GenBank to identify species. All other *Anopheles* mosquitoes were identified by the retrospective correlation of DNA barcodes, with morphologically–verified reference barcodes compiled by Walter Reed Biosystematics Unit and the Mosquito Barcoding Initiative in Y-ML's lab. Head-thorax portions of all samples were separated and used for DNA extraction using the Autogen® automated DNA extraction protocol. MtDNA COI barcodes were amplified using the universal LCO1490 and HCO2198 barcoding primers[40], and amplified, cleaned and bi-directionally sequenced according to previously detailed conditions[41]. All DNA barcodes generated from this study are available under the project "MALAN – Windborne *Anopheles* migrants in Mali" on the Barcode of Life Database (www.boldsystems.org) and in GenBank under accession numbers MK585944–MK586043. *Plasmodium* infection status was determined following previously described protocol[42] using DNA extracts from the whole body for *An. coluzzii* and, for all other specimens, for thorax and head (n=190) as well as separated abdomens (n=156) extracted and tested individually using published protocols[43,44]. Due to the nature of the collections, all body parts were not available for each specimen, accounting for the discrepancy in numbers. Bloodmeal identification was carried out following published protocol[45].

Data Analysis Although aerial collections started in April 2012, protocol optimization and standardization took most of that year, and data included in the present analysis covers only the period March 2013–November 2015. Nights when operations were interrupted by storms or strong winds (e.g., the balloon was retrieved during darkness) were also excluded.

The total number of mosquitoes per panel represents 'net density' of each species. Aerial density was estimated based on the species' panel density and total air volume that passed through that net that night, i.e.,

Aerial density = panel density / volume of air sampled, and

volume of air sampled = panel surface area * mean nightly wind speed * sampling duration,

Net surface area was 3 m^2. Wind speed data were obtained from the atmospheric re-analyses of the global climate, ERA5. Hourly data available at 31 km surface resolution with multiple vertical levels including ground, 2, 10, 32, 55, 85, 115 180, 215, 255, and 300 m agl. Overnight records (18:00 through 06:00) for the nearest grid center were used to calculate the nightly direction and mean wind speed at each village: Siguima, Markabougou and Thierola. Dallowere, located 25 km south of Thierola, was included in the same grid cell of Thierola. The mean nightly wind speed at panel height was estimated based on the nearest available altitude layer.

To evaluate clustering in mosquito panel density and the effects of season, panel height, year and locality, mixed linear models with either Poisson or negative binomial error distributions were implemented by proc GLIMMIX[46]. The clustering at the levels of the panel and the night of sampling were evaluated as random effects as was the case for the year of sampling and locality. These models accommodate counts as non-negative integer values. The ratio of the Pearson χ^2 to the degrees of freedom was used to assess overall "goodness of fit" of the model, with values of >2 indicating a poor fit. The significance of the scale parameter estimating k of the negative binomial distribution was used to choose between Poisson and negative binomial models. Sequential model fitting was used, starting with random factors before adding fixed effects. Lower Bayesian Information Criterion (BIC) values and the significance of the underlying factors were also used to select the best fitting model of each species.

The magnitude of windborne migration was expressed as the expected minimum number of migrants per species crossing an imaginary line of 1 km perpendicular to the wind at altitude. This commonly used measure of abundance assumes that the insects fly in a layer that is 1 km wide and does not require knowledge of the distance or time the insects fly to or from the interception point[47–49]. We used the mean wind speed at altitude (4.8 m/s, see below) and assumed that mosquitoes fly in a layer depth of 200 m between 50 and 250 m agl, conservatively reflecting that mosquitoes were captured between 40-290 m (see below). Accordingly, this nightly migration intensity was computed as the product of the mean aerial density across the year (conservatively including periods when no migrants were captured) by the volume of air passing over the reference line during the night. The corresponding annual index was estimated by multiplying the nightly index by the period of windborne migration estimated from the difference between the first and last day and month a species was captured over the three years. Species that were captured once were assumed to migrate during a single month. The annual number of migrants per species crossing a line of 100 km was used because of the similar species composition across our sampling sites spanning 100 km (Fig. S1a and see below).

Like most insects in their size range[48,50,51], the flight speed of mosquitoes does not typically exceed 1 m/s[52,53]. Because winds at panel altitude attain speeds considerably higher than the mosquito's own speed, flight direction and speed are governed by the wind[47,48] and thus, flight trajectory can be simulated based

on the prevailing winds during the night of capture at the relevant locations and altitudes as has been done previously[54–56]. Accordingly, backward flight trajectories of mosquitoes were simulated using HYSPLIT: Hybrid Single-Particle Lagrangian Integrated Trajectory model[25] based on ERA5 meteorological reanalysis data. Data available in ERA5 present the highest spatial and temporal resolution available for that region. Comparisons with the lower spatial and temporal resolution data available from the MERRA2 reanalysis data[57] and the Global Data Assimilation System available at 0.5 degree spatial resolution showed good agreement in trajectory direction and overall distance (not shown). Trajectories of each captured mosquito were simulated starting at its capture location, altitude, and all multiple interception (full) hours during the night of the collection. Because anophelines are nocturnal, we conservatively assumed that flights started at or after 18:00 and ended by 06:00 the following morning and computed trajectories for every hour that allowed for a total of two or nine h flight. For example, to complete 9 hours flight by 06:00, a mosquito could have started at 18:00, 19:00, 20:00, or 21:00. Total flight duration of tethered female *An. gambiae* s.l. and *An. atroparvus* reached or exceeded 10 hours with average speed of 1 km/h[52] in accord with other studies[53,58,59]. Likewise, *An. vagus* and *An. hyrcanus* caught 150 m agl after midnight over India would have been migrating for >6 hours, assuming they took off around dusk[20]. Thus, we conservatively assumed that windborne long-distance migrant anopheline mosquitoes fly between two and nine hours per night although longer duration is possible. Each trajectory consisted of the global positions of the mosquitoes at hourly intervals from the interception time. In addition to plotting trajectories[60–67], the linear distance from the interception site and the azimuth (angle between interception site and mosquito simulated position from the North, projected on a plane) were computed for all trajectories. To evaluate distance range and dominant directions of flight, the mean and 95% CI of the distance and azimuth (as a circular statistic) were computed for the two- and nine-hours flight trajectories. The dispersion of individual angles (azimuths) around the mean was measured by the mean circular resultant length 'r', which can vary from 0 to 1, with higher values indicating tighter clustering around the mean. Rayleigh's test was used to test that there was no mean direction, as when the angles form a uniform distribution over a circle[68].

Data and Code Availability

1. Data on anopheline capture, identification, sex, and gonotrophic status are available from www.boldsystems.org (Project code: MALAN) and in Genbank (MK585944–MK586043).

2. SAS code used for statistical analyses (and data manipulations) and 9-hour backward trajectories data for each mosquito capture event based on HYSPLIT are available from TL upon request.

3. Plotting trajectories (code available at https://github.com/benkraj/anopheles-migration)

References (Methods and Extended Data)

32. Lehmann, T. *et al.* Tracing the origin of the early wet-season *Anopheles coluzzii* in the Sahel. *Evol. Appl.* **10,** 704–717 (2017).

33. Lehmann, T. *et al.* Seasonal Variation in Spatial Distributions of *Anopheles gambiae* in a Sahelian Village: Evidence for Aestivation. *J. Med. Entomol.* **51,** 27–38 (2014).

34. Huestis, D. L. *et al.* Seasonal variation in metabolic rate, flight activity and body size of *Anopheles gambiae* in the Sahel. *J Exp Biol* **215,** 2013–2021 (2012).

35. Fritz, G. N., Fritz, A. H. & Vander Meer, R. K. Sampling high-altitude and stratified mating flights of red imported fire ant. *J Med Entomol* **48,** 508–512 (2011).

36. Fanello, C., Santolamazza, F. & della Torre, A. Simultaneous identification of species and molecular forms of the *Anopheles gambiae* complex by PCR-RFLP. *Med Vet Entomol* **16,** 461–464 (2002).

37. Scott, J. A., Brogdon, W. G. & Collins, F. H. Identification of single specimens of the Anopheles gambiae complex by the polymerase chain reaction. *Am.J.Trop.Med.Hyg.* **49,** 520–529 (1993).

38. Santolamazza, F. *et al.* Insertion polymorphisms of SINE200 retrotransposons within speciation islands of *Anopheles gambiae* molecular forms. *Malar. J.* **7,** 163 (2008).

39. Simon, C. *et al.* Evolution, Weighting, and Phylogenetic Utility of Mitochondrial Gene Sequences and a Compilation of Conserved Polymerase Chain Reaction Primers. *Ann. Entomol. Soc. Am.* **87,** 651–701 (1994).

40. Folmer, O., Black, M., Hoeh, W., Lutz, R. & Vrijenhoek, R. DNA primers for amplification of mitochondrial cytochrome c oxidase subunit I from diverse metazoan invertebrates. *Mol. Mar. Biol. Biotechnol.* **3,** 294–9 (1994).

41. Linton, Y.-M. *et al.* Mosquitoes of eastern Amazonian Ecuador: biodiversity, bionomics and barcodes. *Mem. Inst. Oswaldo Cruz* **108 Suppl 1,** 100–9 (2013).

42. Bass, C. *et al.* PCR-based detection of Plasmodium in Anopheles mosquitoes: a comparison of a new high-throughput assay with existing methods. *Malar. J.* **7,** 177 (2008).

43. Demas, A. *et al.* Applied Genomics: Data Mining Reveals Species-Specific Malaria Diagnostic Targets More Sensitive than 18S rRNA. *J. Clin. Microbiol.* **49,** 2411–2418 (2011).

44. Steenkeste, N. *et al.* Towards high-throughput molecular detection of *Plasmodium*: new approaches and molecular markers. *Malar. J.* **8,** 86 (2009).

45. Kent, R. J. & Norris, D. E. Identification of mammalian blood meals in mosquitoes by a multiplexed polymerase chain reaction targeting cytochrome B. *Am. J. Trop. Med. Hyg.* **73,** 336–42 (2005).

46. SAS Inc., I. SAS for Windows Version 9.3. (2011).

47. Hu, G. *et al.* Mass seasonal bioflows of high-flying insect migrants. *Science (80-.).* **354,** 1584–1587 (2016).

48. Drake, V. A. & Reynolds, D. R. *Radar entomology : observing insect flight and migration*. (CABI International., 2012).

49. Reynolds, D., Chapman, J. & Stewart, A. Windborne migration of Auchenorrhyncha (Hemiptera) over Britain. *Eur. J. Entomol.* **114,** 554–564 (2017).

50. Taylor, L. R. Insect migration, flight periodicity and the Boundary Layer. *J. Anim. Ecol.* **43,** 225–238 (1974).

51. Chapman, J. W., Drake, V. A. & Reynolds, D. R. Recent Insights from Radar Studies of Insect Flight. *Annu. Rev. Entomol. Vol 56* **56,** 337–356 (2011).

52. Kaufmann, C. & Briegel, H. Flight performance of the malaria vectors *Anopheles gambiae* and *Anopheles atroparvus*. *J. vector Ecol.* **29,** 140–153 (2004).

53. Snow, W. F. Field estimates of the flight speed of some West African mosquitoes. *Ann. Trop. Med. Parasitol.* **74,** 239–242 (1980).

54. Eagles, D., Walker, P. J., Zalucki, M. P. & Durr, P. A. Modelling spatio-temporal patterns of long-distance Culicoides dispersal into northern Australia. *Prev. Vet. Med.* **110,** 312–322 (2013).

55. Stefanescu, C., Alarcón, M. & Àvila, A. Migration of the painted lady butterfly, *Vanessa cardui*, to north-eastern Spain is aided by African wind currents. *J. Anim. Ecol.* **76,** 888–898 (2007).

56. Klausner, Z., Fattal, E. & Klement, E. Using synoptic systems' typical wind trajectories for the analysis of potential atmospheric long-distance dispersal of lumpy skin disease virus. *Transbound. Emerg. Dis.* **64,** 398–410 (2017).

57. Gelaro, R. *et al.* The Modern-Era Retrospective Analysis for Research and Applications, Version 2 (MERRA-2). *J. Clim.* **30,** 5419–5454 (2017).

58. Pedgley, D. E. *Windborne pests and diseases: Meteorology of airborne organisms*. (Ellis Horwood Ltd., 1982).

59. Gillies, M. T. & Wilkes, T. J. Field experiments with a wind tunnel on the flight speed of some west African mosquitoes (Diptera: Culicidae). *Bull. Entomol. Res.* **71,** 65 (1981).

60. Kahle, D. & Wickham, H. ggmap: Spatial Visualization with ggplot2. *R J.* **5,** 144–161 (2013).

61. Hijmans, R. J. geosphere: Spherical Trigonometry. (2017).

62. Slowikowski, K. ggrepel: Automatically Position Non-Overlapping Text Labels with 'ggplot2'. (2018).

63. Santos Baquero, O. ggsn: North Symbols and Scale Bars for Maps Created with 'ggplot2' or 'ggmap'. (2019).

64. Arnold, J. B. ggthemes: Extra Themes, Scales and Geoms for 'ggplot2'. (2019).

65. Grolemund, G. & Wickham, H. Dates and Times Made Easy with {lubridate}. *J. Stat. Softw.* **40,** 1–25 (2011).

66. RStudio Team. RStudio: Integrated Development Environment for R. (2015).

67. R Core Team. R: A Language and Environment for Statistical Computing. (2016).

68. Fisher, N. I. *Statistical Analysis of Circular Data.* (Cambridge University Press, 1993).

Extended Data Figure 1. Study area and aerial sampling effort. a) Map of the study area with aerial sampling villages and the number of sampling nights per village under a schematic map of Africa showing the Sahel region (source: Wikipedia, https://pt.m.wikipedia.org/wiki/Ficheiro:Sahel_Map-Africa_rough.png). **b**) Nightly sampling effort by year. Fringe under zero indicates the sampling nights (by village) and needles denote the total number of mosquitoes per night regardless of the number of panels per night. Dry and wet seasons are indicated by yellow and green in the ruler under the X-axis.

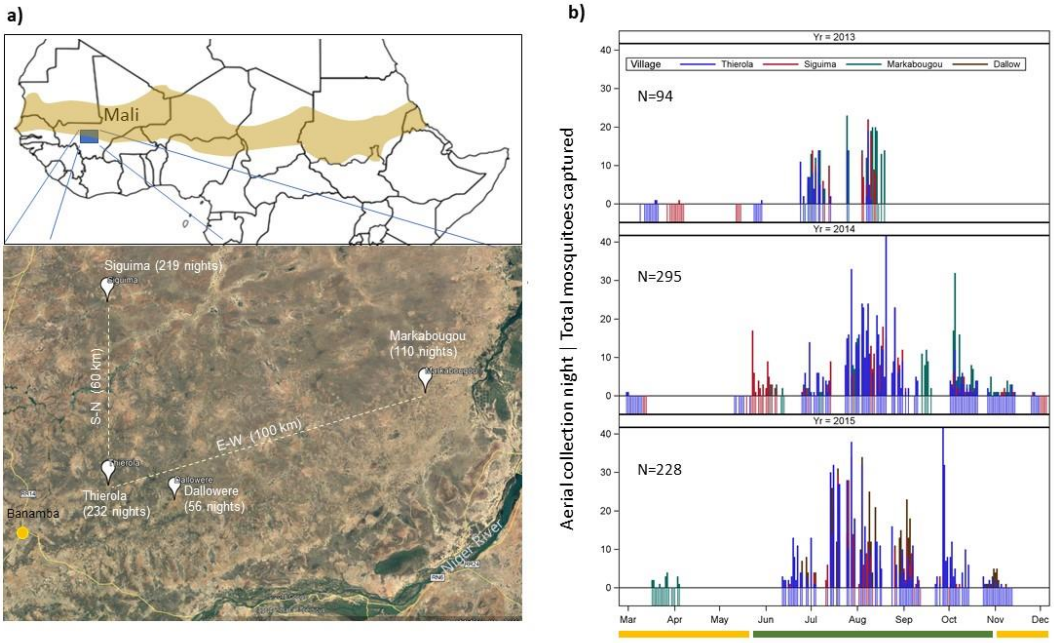

Extended Data Figure 2. Regularity of migratory flights, flight altitude, and variability among years and localities in species aerial presence. a) Relationship between mosquito presence (fraction of positive nights) and mean panel density to evaluate if appearance can be accounted by overall abundance rather than by unique migratory nights. **b)** The relationship between panel height and mean mosquitoes density/panel (x10^3, regression line with shading denotes 95% CI) showing mean panel density by species. Inset summarizes the covariance analysis (ANCOVA), underlying this regression, which includes the species and panel height. Number of nights per panel altitude is given in blue along the X axis (see Figure 1a). **c)** Variation in mosquito presence (fraction of positive nights) by species between years (top) and villages (bottom) with their 95% CI. Sampling effort expressed as the number of panels per year/village is shown adjacent to the legend.

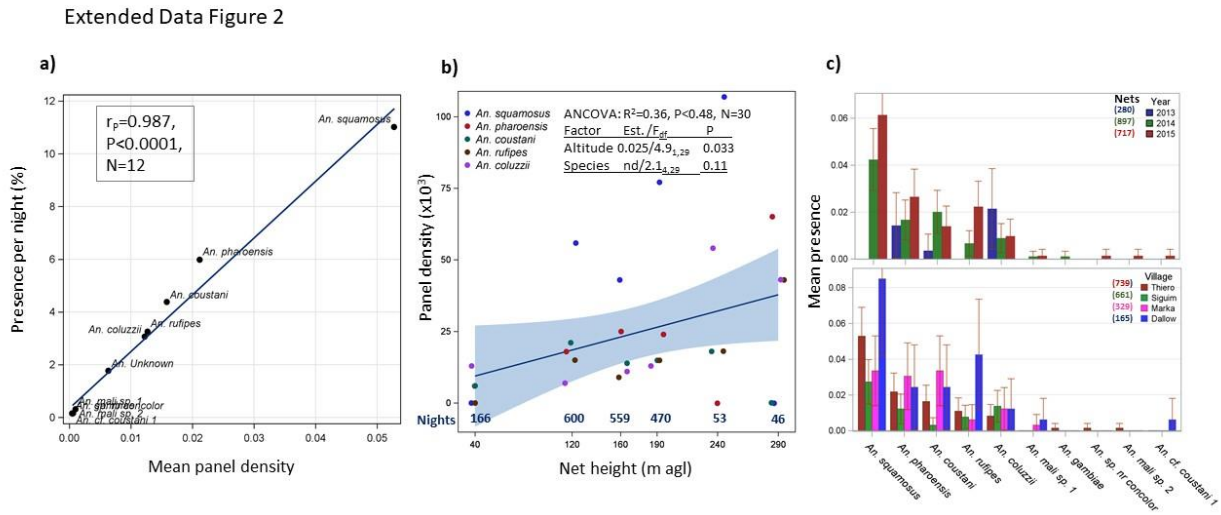

Extended Data Table 1. Variation in mosquito capture rate between years, localities, and heights above ground (GLIMMIX models of random and fixed variables, total number of panels was 1,894).

Dependent: Panel Density	Parameter	*A. squamosus*	*A. pharoensis*	*A. coustani*	*A. rufipes*	*A. coluzzii*
Random vars only: Poisson	Pearson $\chi 2$/df (BIC)	1.13 (793.5)	**1.04 (394.4)**	**0.90 (306.52)**	**1.11 (260.4)**	**1.16 (252.8)**
Random vars only:	Pearson χ^2/df, Scale[a] (BIC)	**0.83, 5.98*** (756.2)**	0.97, 3.84^{ne} (391.4)	0.87, 2.09^{ns} (306.7)	0.99, 10.6^{ne} (254.5)	0.98, 15^{ns} (246.7)
Negative Binomial	intercept[mean] (SD)	-4.06^{ns} (1.23)	-3.9** (0.226)	-4.4* (0.63)	-4.7*** (0)	-4.4** (0.23)
	Year (SD)	3.24^{ns} (4.36)	0^{ns} (0.06)	0.09^{ns} (0.31)	0.55^{ns} (0.56)	0^{ne}
	Locality[b] (SD)	0.075^{ns} (0.116)	0.04^{ns} (0.15)	0.73^{ns} (3.19)	0^{ne}	0^{ne}
Random vars only: Poisson	Night[c] (SD)	**4.02** (1.42)**	**1.78* (0.99)**	6.57^{ns} (7.3)	**29.0* (16.8)**	**32.0* (17.9)**
Random vars only: Neg. Bin.	Night[c] (SD), scale	3.9** (1.5), 0.74^{ns}	1.6^{ns} (1.1), 0.34^{ns}	0.5^{ne} (ne), 0^{ne}	30.1* (17.5), 0.7^{ns}	33.5* (18.7), 0.76^{ns}
Fixed and random: Poisson	Pearson χ^2/df (BIC)	0.37 (700)	0.6 (403)	0.2 (308)	0.09 (258)	0.08 (243)
	Night	1.4** (0.0)	0.78^{ns} (0.8)	1.9* (1.1)	14.0^{ns}(13.3)	21.9^{ns} (15.2)
	Period[d]	Aug-Oct*	Aug-Oct*	Aug-Oct^{ns}	Aug-Oct^{ns}	Aug-Oct***
	Panel height (m)	0.001***(0)	0.003***(0)	-0.007***(0)	0.001***(0)	0.014*(0.006)
Dependent: Aerial Density	Pearson χ^2/df (BIC)	0.42 (938)	0.41 (503)	0.2 (378)	0.1 (304)	0.09 (283)
Fixed and random: Poisson	Night	2.9*** (0.8)	2.6* (1.2)	5.2^{ns} (3.9)	26.8*(16.0)	31.5* (17.6)
	Period[d]	Aug-Oct^{ns}	Aug-Oct*	Aug-Oct^{ns}	Aug-Oct^{ns}	Aug-Oct***
	Panel height (m)	-0.003***(0)	-0.002***(0)	-0.008*(0.004)	-0.001***(0)	0.01*(0.005)

[a] - For negative bionomial scale parameter estimates the k parameter of this distribution.

[b] - The effects locality was estimated considering only 3 locations after pooling Dallowere and Thierola which are only 20 km apart (see Methods).

[c] The significance of clustering by night (across locations) estimated as the only random effect (using subject statement) after finding insignificant variance componenets of Year and Location.

[d] Periods included: March-May, June-July, August-October, and November-December. The period of highest panel density is shown with its statistical significance.

[e] Panel height levels inlcuded 40, 120 (90-120), 160, 190, and 250, (220-290) m agl due to small sample sizes (nights) of certain altitudes.

***, **,*, ^{ns}, and ^{ne} refer to significance probability of 0.001, 0.01 and 0.05, >0.05, and to parameters that could not be estimated, respectively.

Extended Data Figure 3. A photo showing a tethered sticky panel setup and attachment. A sticky panel (3x1m net) on a test helium balloon (lower volume/capacity), showing attachment of net covered with glue to the cord tethering the balloon to the ground. Note the four carbon poles and Velcro attachment points (see text for details). A close-up of the attachment of the panel to the cord and preparing to launch a standard 3 m balloon.